



# Elastic seismic inversion with geostatistical information: resolution and application to an AVO class III gas reservoir

Miguel Bosch, Laboratory of Geophysical Simulation and Inversion, Universidad Central de Venezuela

Astrid Torres, Laboratory of Geophysical Simulation and Inversion, Universidad Central de Venezuela

Copyright 2009, SBGf - Sociedade Brasileira de Geofísica

This paper was prepared for presentation during the 11<sup>th</sup> International Congress of the Brazilian Geophysical Society held in Salvador, Brazil, August 24-28, 2009.

Contents of this paper were reviewed by the Technical Committee of the 11<sup>th</sup> International Congress of the Brazilian Geophysical Society and do not necessarily represent any position of the SBGf, its officers or members. Electronic reproduction or storage of any part of this paper for commercial purposes without the written consent of the Brazilian Geophysical Society is prohibited.

## Abstract

In this work we describe a method for joint inversion of multi-angle partial stacks under geostatistical prior constraints for the estimation of the parameters of an isotropic elastic medium. The method is based on fitting the calculated and observed seismic data and minimizing the deviations of the elastic model configuration from the prior configuration, which is obtained by statistical characterization of well-log data. The statistical component of the model correlates vertically (in time) the CDP elastic properties, regularizing the model to the well-log spatial statistics. Lateral property correlations are not included in this work. We define an appropriate measure of the resolving power of the seismic data for spatially correlated models, and illustrate the improvement of the elastic properties resolution with the number of angle stacks considered and the incidence angle range. We show results for a field case, corresponding to a class III gas reservoir, where the mass density and shear velocities estimated from the elastic inversion are key information for the identification of the gas bearing sands.

## Introduction

The goal of seismic inversion is to map seismic reflections into intervallic meaningful physical properties, providing valuable information for fluid and lithology discrimination. Different types of spatial regularization methods are used to constraint the inversion. Common methods are the sparse spike and the Tikonov approaches, among others. The spatial regularization of the property fields imposes a texture (variability and spatial correlation) to the resulting configuration, which should be as realistic as possible. An approach that we follow in this work is to honor the texture and correlations of the elastic fields estimated from well-logs after appropriate transformation to the seismic resolution scale, using standard geostatistical characterization: modeling the covariance and cross-covariance functions.

The issue of spatial regularization is important in the context of seismic inversion, as it is related with the data resolution of the estimated properties. The data resolution concept quantifies the contribution of the data to the estimated configuration. In its original formulation (Backus and Gilbert, 1968), it measures the proportion of a true model perturbation that is mapped into the estimated

model after the inversion of the corresponding calculated data. The data resolution depends (Bosch et al., 2005) on the spatial model regularization. In general the data resolution is larger when the model regularization is commensurable with the information scale content of the observed data.

## Elastic seismic inversion

In a statistical framework the seismic inversion result is modeled with a posterior probability density defined over the model parameter space,

$$\sigma(\mathbf{m}) = c L(\mathbf{m}) \rho(\mathbf{m}), \quad (1)$$

where  $L(\mathbf{m})$  is the seismic likelihood function and  $\rho(\mathbf{m})$  the prior probability density for the model parameters. Here, we describe the elastic isotropic medium with the mass density, compressional velocity and shear velocity, defined in a sequence of horizontal layers of equal travel time. Thus, our model parameters array,  $\mathbf{m}$ , have here  $3 \times N$  dimensions, with  $N$  being the number of layers at the CDP model. For each CDP location we solve for the model parameters that maximize the probability density. The seismic likelihood measures the proximity between the observed seismic data and the corresponding calculated seismic data. The seismic data is calculated by a convolutional model using Zoeppritz equations and compared with partial angle stacks obtained from the seismic data.

We model the prior information with a multivariate Gaussian joint probability density on the model parameter space,

$$\rho(\mathbf{m}) = \exp[-1/2 ((\mathbf{m} - \mathbf{m}_{\text{prior}})^T \mathbf{C}_m^{-1} (\mathbf{m} - \mathbf{m}_{\text{prior}}))], \quad (2)$$

with  $\mathbf{m}_{\text{prior}}$  being the prior model for the elastic parameters and  $\mathbf{C}_m$  the model covariance matrix. For the definition of the model covariance we fully characterize the covariance and cross-covariances of upscaled well-log derived elastic properties: here, the mass density, compressional and shear seismic velocities.

To solve for the maximum probability model configuration in expression (1) we apply the Newton's method, obtaining the expressions,

$$\begin{cases} \mathbf{A} = (\mathbf{I} + \mathbf{C}_m \mathbf{G}^T \mathbf{C}_d^{-1} \mathbf{G}), \\ \mathbf{b} = \mathbf{m}_{\text{prior}} - \mathbf{m} + \mathbf{C}_m \mathbf{G}^T \mathbf{C}_d^{-1} (\mathbf{d}_{\text{obs}} - \mathbf{d}_{\text{calc}}), \\ \mathbf{A} \Delta \mathbf{m} = \mathbf{b}, \end{cases} \quad (3)$$

for the curvature matrix  $\mathbf{A}$ , the steepest ascent direction  $\mathbf{b}$ , and the equation for the model update  $\Delta \mathbf{m}$ . Above,  $\mathbf{C}_d$ , is the data covariance matrix,  $\mathbf{I}$  is the identity matrix, and  $\mathbf{G}$ , is the matrix of the derivatives of the calculated data

with respect to the model parameters. As the model to data relationships are non linear, expression (3) is solved iteratively until convergence.

**Uncertainty and data resolution**

In the neighborhood of the optimal model, the posterior covariance matrix is given by,

$$C_m^{post} = A^{-1} C_m, \quad (4)$$

and the seismic data resolution power matrix for a model local perturbation honoring the prescribed covariance is (Bosch, 2005),

$$P_{seis} = A^{-1} R_m^{1/2}, \quad (5)$$

where  $R_m^{1/2}$  is a square root of the prior model correlation matrix, i.e. the standardized square root of the prior model covariance matrix. The diagonal elements of the posterior covariance are the variance of the estimated model parameters. The diagonal elements of the seismic resolution power matrix are in the range [0,1] and indicate the contribution of the seismic data to the property estimation. As a complement, the prior model resolution power matrix is,  $P_{mod} = I - R_{seis}$ , where  $I$  is the identity matrix.

Figure 1 shows in two synthetic tests the effect of the model time correlation in the posterior uncertainty and seismic resolution power, using the above seismic inversion formulation. For these examples we co-simulate the mass density, compressional and shear velocities according to a particular geostatistical model (mean trend and covariance for the model series in time) and proceed with the geostatistical inversion of the calculated seismic data, with the same geostatistical parameters. In figure 1a we used a Gaussian covariance function with 20 ms range for Vp and 100 ms range for Vs and density. In figure 1b we show results of a rougher property model corresponding to mixed nugget effect and Gaussian covariance models with 20 ms range for the three properties. The figure shows that in the smoother time profile case, figure 1a, the posterior uncertainty is smaller and the seismic data resolution power higher than in the second case. The source seismic wavelet and the incidence angles considered are the same in the two cases.

A better recognized effect on the improvement of the precision and data resolution power in elastic seismic inversion is related with the angle range and the number of partial angle stacks considered in the inversion. Figures 2a, 2b and 2c show the cases of one, two and eight angles considered for the same geostatistical parameters as in figure 1a, which was obtained with the inversion of three incidence angles data. From these examples we confirm that the elastic inversion of seismic reflection data is effective for the estimation of the shear velocity and mass density if an appropriate angle sampling is done. On the other hand, the resolution and accuracy of the compressional velocity estimation is commonly larger than for the other two properties considered

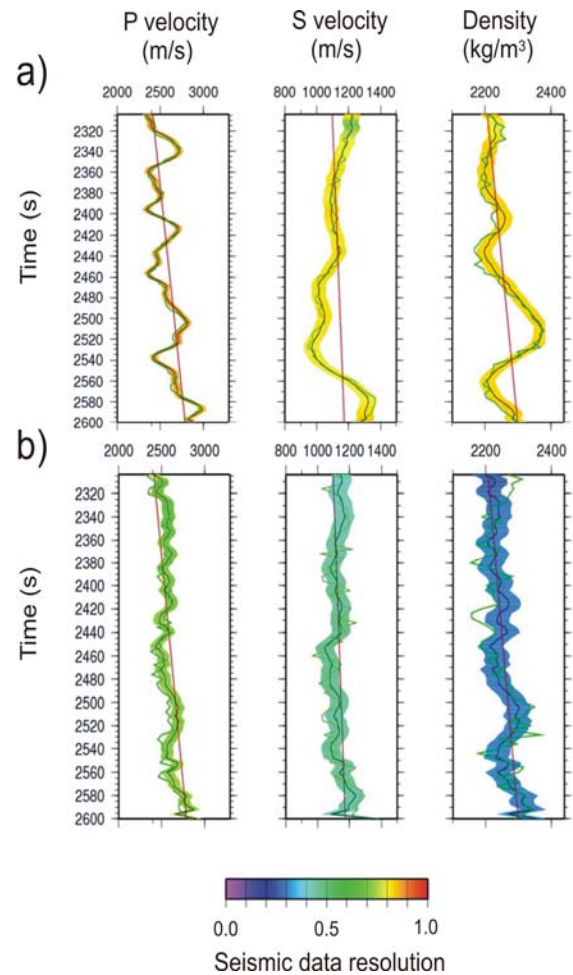


**Figure 1:** Synthetic tests for the estimation of the compressional velocity, seismic velocity and density from the inversion of three incidence angle seismic data (15°, 30° and 50°) for target models honoring different time covariance functions: property profiles are smoother in case (a) than in case (b). The prior profiles (red), the target profiles (green) and the estimated profiles (black) are shown for each property plot. The thickness of the bands describes the posterior uncertainty in ± 1 standard deviation and the color indicates the seismic data resolution power.

**Field example**

We applied the method to field data in a gas reservoir. The gas reservoir produces a large reflection with AVO effect typical of a class III reservoir. However, other strong reflections are also present, which result from lithological changes. Also the continuity of the gas bearing sands was one of the issues to explore.

For the application to the field case, we characterize the covariance of the mass density, compressional and shear velocities obtained from well-log data. First, these properties were upscaled from the original well-log sampling to the appropriate time sampling at the seismic resolution. Considering the frequency content we

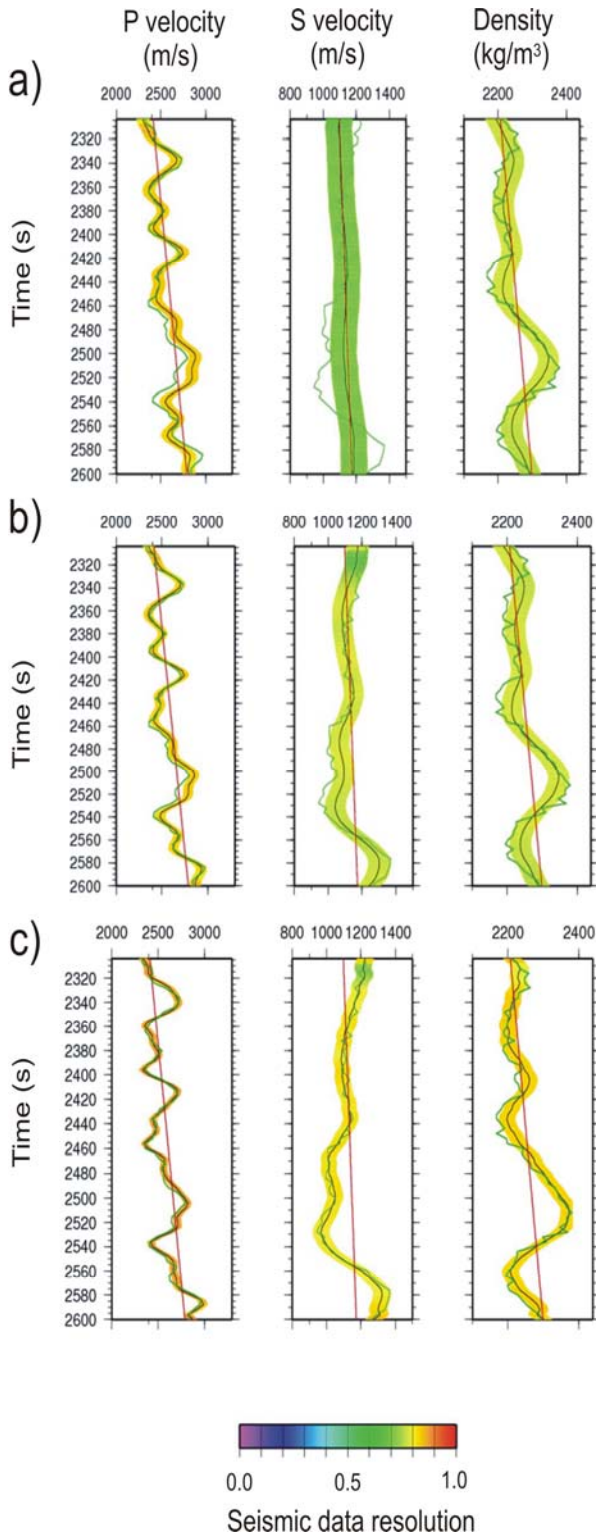


**Figure 2:** Synthetic tests results for the compressional velocity, seismic velocity and density corresponding to the same target model inverted in Figure 1a. In these cases the elastic parameters are jointly estimated with the inversion of: (a) one incidence angle seismic data of 30°, (b) two angles data of 15° and 30°, and (c) eight angles data of 11°, 15°, 30°, 25°, 35°, 40°, 50° and 55°. Plots description is the same as in Figure 3.

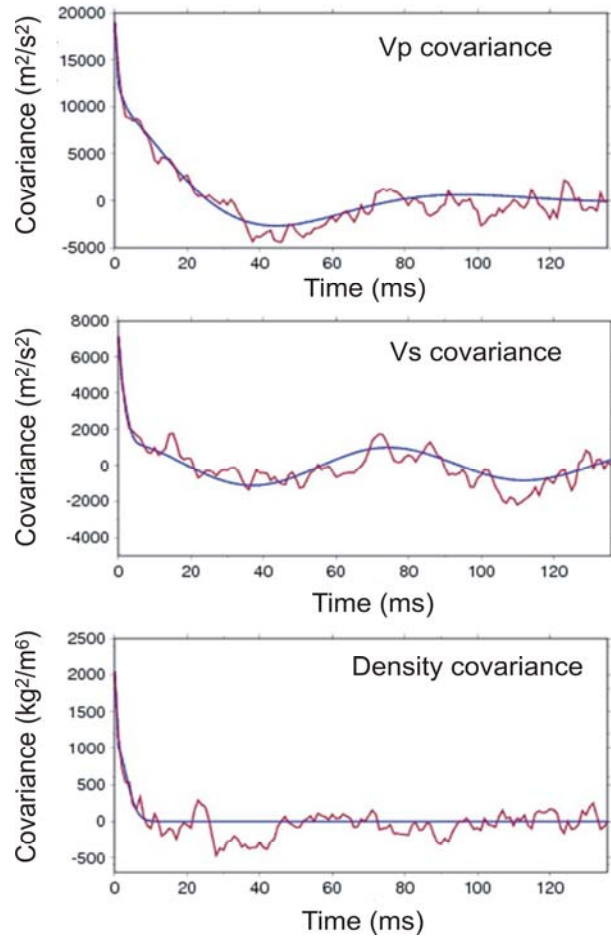


**Figure 3:** Experimental covariance (red line) calculated from the upscaled well-log derived compressional velocity, shear velocity and mass density, and the covariance function models (blue line) fitted to the covariance data.

modeled the medium with 4 ms TWT layers, which correspond approximately to a quarter of the dominant seismic signal period. Upscaling the mass density follows plain average in depth. However, the velocity upscaling requires Backus average. Figure 3 shows the experimental covariance of the upscaled properties and the corresponding modeled covariance functions. The cross-covariances were also modeled. The covariance functions are fitted by a regression procedure to the experimental covariance data and used in the construction of the model covariance matrices in expressions (2-5). A similar geostatistical well-log data characterization is done by Bosch et al. (2007) in the context of an oil reservoir.

We inverted the seismic data in three partial stacks for angle ranges centered at 15°, 30° and 40° to jointly estimate the mass density, compressional and shear velocity fields. From the three properties, we also reconstructed several elastic modulus and ratios of common interest. Among the different elastic parameters, we found that the mass density was particularly useful in this area for the identification of the gas reservoir,



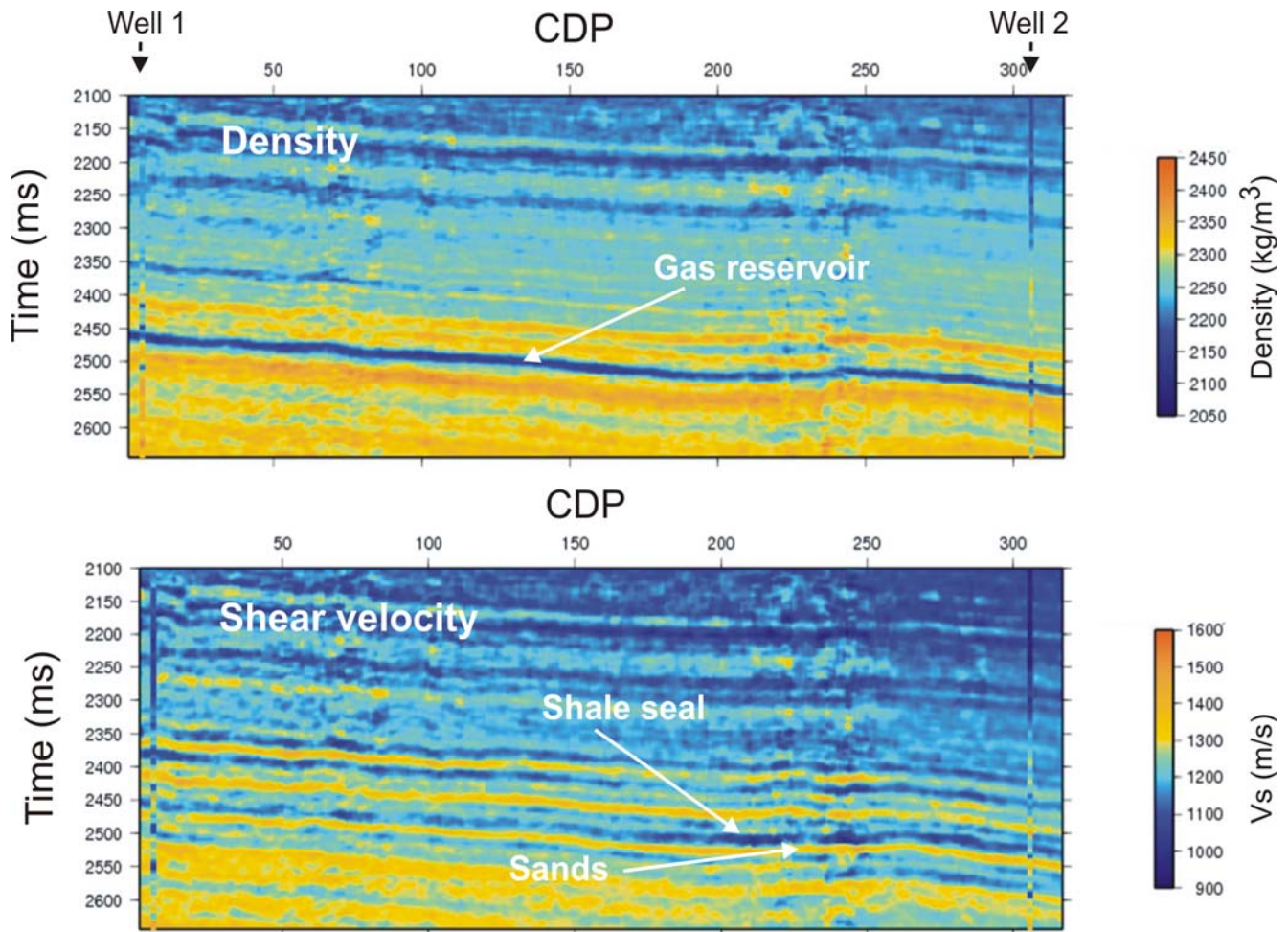


**Figure 4:** Density and shear velocity estimated with the elastic inversion for a time window including the reservoir stratum. The corresponding properties calculated from the well-log data and upscaled to seismic resolution are superposed at the locations of two wells for comparison with the inversion results.

characterized by low density. On the other hand, the shear wave velocity correlated well with lithology in the area: high shear velocities in sands and low shear velocities in shale. Figure 4 shows the mass density and shear velocity estimated from the elastic inversion with indications of the reservoir location. Well-log derived mass density and shear velocity are superposed at the location of two wells for comparison.

**Conclusion**

Elastic seismic inversion is a useful tool in reservoir characterization as it maps seismic amplitudes to elastic medium properties, related to lithology, fluid and porosity. We improve common formulation of the elastic seismic inversion with the definition of an adequate geostatistical model for the elastic medium properties based on detailed modeling of well-log derived elastic parameters. This characterization is done at a scale commensurable with the seismic signal. The geostatistical model regularizes in a realistic manner the elastic property model. In addition to compressional seismic velocity, shear velocities and densities are reliably estimated by the elastic inversion

method, and have a relevant contribution to the reservoir characterization.

**Acknowledgements**

We thank the CDCH-UCV (PG-0800-5631-2008), Jesús Sierra (IGS Consulting Services), Milagrosa Aldana (USB) and Eni for their contribution to this work.

**References**

**Backus, G., and F. Gilbert,** 1968, The resolving power of gross Earth data: *Journal of the Royal Astronomical Society*, 16, 169-205.

**Bosch, M., L. Cara, J. Rodrigues, A. Navarro and M. Díaz,** 2007, A Monte Carlo approach to the joint estimation of reservoir and elastic parameters from seismic amplitudes, *Geophysics*, 72, 6, O29-O39.

**Bosch, M., P. Barton; S. Singh, and I. Trinks,** 2005, Inversion of traveltme data under a statistical model for seismic velocities and layer interfaces, *Geophysics*, 70, 4, R33-R43.